



# 1 Tsunami damage to ports: Cataloguing damage to create fragility 2 functions from the 2011 Tohoku event

3  
4 Constance Ting Chua <sup>1,2</sup>, Adam D. Switzer <sup>1,2</sup>, Anawat Suppasri <sup>3</sup>, Linlin Li <sup>4</sup>, Kwanchai Pakoksung <sup>3</sup>,  
5 David Lallemand <sup>1,2</sup>, Susanna F. Jenkins <sup>1,2</sup>, Ingrid Charvet <sup>5</sup>, Terence Chua <sup>1</sup>, Amanda Cheong <sup>6</sup> and Nigel  
6 Winspear <sup>7</sup>

7  
8 <sup>1</sup> Asian School of the Environment, Nanyang Technological University, Singapore

9 <sup>2</sup> Earth Observatory of Singapore, Nanyang Technological University, Singapore

10 <sup>3</sup> International Research Institute of Disaster Science, Tohoku University, Sendai, Japan

11 <sup>4</sup> School of Earth Sciences and Engineering, Sun Yat-Sen University, Guangzhou, China

12 <sup>5</sup> Formerly Department of Statistical Science, University College London, London, United Kingdom

13 <sup>6</sup> JBA Risk Management Pte Ltd, Singapore

14 <sup>7</sup> Formerly SCOR Global P&C, Singapore

15

16 *Correspondence to:* Constance Chua (CCHUA020@e.ntu.edu.sg)

17 **Abstract.** Modern tsunami events have highlighted the vulnerability of port structures to these high-impact but infrequent  
18 occurrences. However, port planning rarely includes adaptation measures to address tsunami hazards. The 2011 Tohoku  
19 tsunami presented us with an opportunity to characterise the vulnerability of port industries to tsunami impacts. Here, we  
20 provide a spatial assessment and photographic interpretation of freely available data sources. Approximately 5,000 port  
21 structures were assessed for damage and stored in a database. Using the newly developed damage database, tsunami damage  
22 is quantified statistically for the first time, through the development of damage fragility functions for eight common port  
23 industries. In contrast to tsunami damage fragility functions produced for buildings from existing damage database, our  
24 fragility functions showed higher prediction accuracies (up to 75% accuracy). Pre-tsunami earthquake damage was also  
25 assessed in this study, and was found to influence overall damage assessment. The damage database and fragility functions for  
26 port industries can inform structural improvements and mitigation plans for ports against future events.

27



## 28 1. Introduction

29 Port assets are vulnerable to the physical damage caused by tsunamis and cascading effects such as extensive supply chain  
30 disruption. For example, transoceanic waves from the 2004 Indian Ocean tsunami resulted in heavy damage to maritime  
31 facilities across the Indian Ocean. On the west coast of Banda Aceh, Indonesia, all harbours and landing piers between Lhok  
32 Nga and Meulaboh were destroyed and unusable (Janssen, 2005) and across the Indian Ocean, heavy damage to maritime  
33 facilities reportedly resulted in the closure of Nagappattinam Port, India for weeks (Mahshwari et al., 2005). On the same note,  
34 the 2011 Tohoku (Great East Japan) tsunami caused damage to many ports along the Pacific coast in the Tohoku region. The  
35 affected ports suffered from a contraction in export and import values following the tsunami (March – May 2011) of 57.5%  
36 and 61.6% respectively, relative to the preceding 5-year average for the same period (Japan Maritime Centre, 2011). Total  
37 economic losses for tsunami damage to Japan's marine vessels, ports and maritime facilities were approximated at US\$ 12  
38 billion (Muhari et al., 2015). A recent study speculated that earthquakes greater than Mw 8.5 from the Manila-trench could  
39 result in the loss of functions in up to five major ports including Kaohsiung and Hong Kong (Otake et al., 2019). Additionally,  
40 threats from future tsunami events are expected to be exacerbated by rising sea levels (Li et al., 2018), which imply greater  
41 risks for port assets located near tsunami sources.

42 With about 80% of global trade volume carried by sea, ports are critical nodes in international trade. Ports are also home to  
43 industrial clusters and critical facilities such as manufacturing firms and power plants due to the convenience they provide.  
44 With increased seaborne trade, globalisation of complex industrial processes and dependence on ports for economic  
45 development, port areas are only expected to develop further. However, port planning rarely accounts for adaptation to natural  
46 hazards and coastal protection structures are usually built to mitigate short-term hazard scenarios such as coastal flooding and  
47 wave damage (Lam and Lassa, 2017).

48 Tsunamis are high-impact events but infrequent occurrences, which makes their potential impacts to ports difficult to quantify.  
49 The expected increase in the exposure of port assets to coastal hazards, combined with our limited experience with tsunamis  
50 in modern ports, demonstrates a clear need to better understand how port structures might respond to tsunami impacts.

51 Structural damage resulting from tsunami impacts has generated considerable interest since the 2004 Indian Ocean tsunami  
52 (e.g. Nistor et al., 2010, Leelawat et al., 2016; Song et al., 2017; Suppasri et al., 2019). Structural damage is most commonly  
53 quantified in the form of tsunami damage fragility functions. First developed for tsunami events by Koshimura et al. (2009),  
54 tsunami fragility functions express the probability that a structure exceeds a prescribed damage threshold for a given tsunami  
55 flow characteristic or intensity measure. Pioneering work in the development of tsunami fragility functions has been largely  
56 focused on damage to residential and commercial buildings (e.g. Leone et al., 2011, Reese et al., 2011; Mas et al., 2012; Gokon  
57 et al., 2014). In recent years, the study of tsunami structural fragility has been extended to critical infrastructure such as roads  
58 and bridges (Akiyama et al., 2014; Shoji and Nakamura, 2017; Williams et al., 2020).

59 Despite recent efforts, our understanding of tsunami impacts on ports still falls short. The coverage of tsunami-induced damage  
60 on port structures in existing literature is by and large limited to qualitative assessments. To date most studies on tsunami



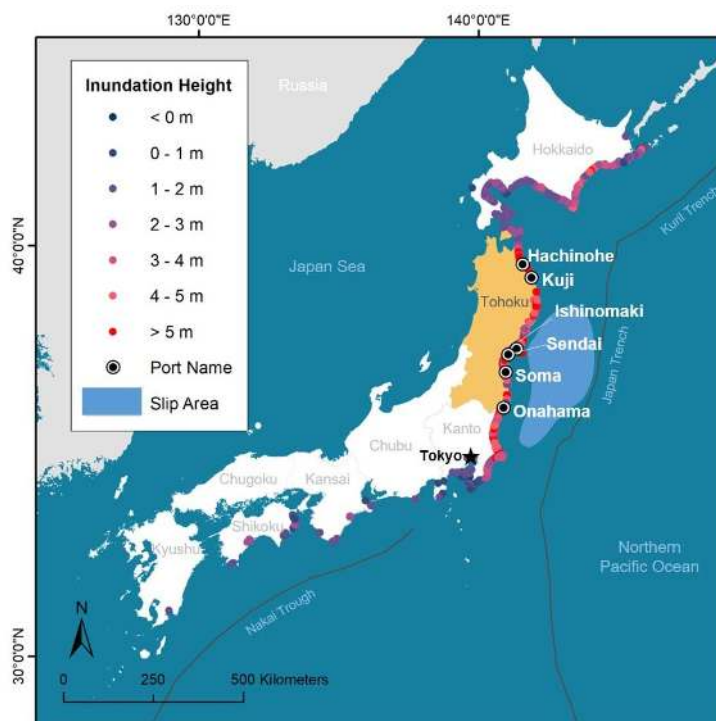
61 structural damage to ports are in the form of post-tsunami surveys, which document damage observations and describe the  
62 failure mechanisms of harbour elements such as breakwaters, quay walls and wharves (e.g. Meneses and Arduino, 2011; Fraser  
63 et al., 2012; Hazarika et al., 2013; Paulik et al., 2019; Benzair et al., 2020) and port facilities such as oil tanks, cranes and  
64 equipment (e.g. Scawthorn et al., 2016; Percher et al., 2013; Sugano et al., 2014). Some studies have attempted to reconstruct  
65 structural impacts to port facilities by evaluating design specifications of structures or examining specific tsunami behaviour  
66 such as bore impact linked to structural damage (e.g. Nayak et al., 2014; Kihara et al., 2015; Chen et al., 2016; Huang and  
67 Chen, 2020). Though recent studies attempted to quantify tsunami damage to port facilities, the focus of these standalone  
68 studies are specific to certain port industries, namely warehousing (Karafa et al., 2018) and fishery industries (Imai et al.,  
69 2019), and therefore do not provide a comprehensive view of the damage sustained by different port industries. While  
70 necessary for the improvement of structural design, efforts so far are not adequate in quantifying tsunami damage statistically.  
71 This study serves as a starting point in characterising the vulnerability of port industries to tsunami impacts, through the  
72 assessment and quantification of structural response to tsunami inundation depths. The objective of this study is two-fold – (i)  
73 to develop a tsunami damage database for port structures impacted during the 2011 Tohoku tsunami, and based on the damage  
74 database, (ii) to construct tsunami damage fragility functions for port industries. The 2011 Tohoku tsunami presents a unique  
75 opportunity to study tsunami damage to port structures due to the extent and severity of damage, and the large ensemble of  
76 data collected post-tsunami (Table 1). The combination of densely recorded tsunami flow measurements, well-documented  
77 surveyed damage data and high-quality photographic evidence available offers an unparalleled resource for this research.  
78 In this paper, we develop the first tsunami damage database for port industries and their related structures. We also present the  
79 first sets of tsunami damage fragility models for common industries found in the port hinterland. We describe the data sources  
80 and methods to develop this damage database, and demonstrate in detail how the damage database addresses limitations found  
81 in past studies. Fragility functions are constructed by reviewing and employing best practices in the field. Unique to this work,  
82 we also evaluated the robustness of tsunami fragility functions against the influence of pre-tsunami earthquake effects. We  
83 conclude by highlighting some key application opportunities of this dataset and providing recommendations for overcoming  
84 current limitations found in this study. This study provides a blueprint for translating post-event damage surveys into fragility  
85 functions, which can be used to forecast future tsunami-induced damage to ports.

## 86 **2. Study site**

87 The northeast coast of Japan, also known as the Tohoku region, was severely impacted by the Tohoku tsunami on 11 March  
88 2011 (Fig. 1). Port operations along the Pacific Coast in Tohoku and eastern Kanto regions were disrupted due to debris and  
89 severe damage to buildings, loading facilities, wharfs, fuel facilities and seawalls (Takano et al., 2012). Damage patterns varied  
90 along the Tohoku coastline. The Tohoku coastline is mainly coastal plains and ria coasts. Coastal plains are extensive areas of  
91 low-lying flat terrain, while ria coasts, formed by submergence of former river valleys, typically have limited flat terrain. Ria  
92 coasts are characterised by narrow funnel-shaped coastal inlets bounded by steep slopes such as mountains. In coastal plains,



93 damage severity transitioned gradually with distance inland, decreasing as inundation depths decrease with distance inland  
94 (De Risi et al., 2017). In ria coasts, the spatial distribution of damage was uneven because flow characteristics i.e. velocity and  
95 hydrodynamic force, which influence damage severity, varied significantly for different points at the same distance inland or  
96 with similar inundation depths (Suppasri et al., 2013; De Risi et al., 2017). This was due to the differences in local topography  
97 (Tsuji et al., 2014). Coastal topography influences tsunami behaviour on land, and therefore influences tsunami flow dynamics  
98 and inundation characteristics (Suppasri et al., 2015). Previous studies have highlighted the importance of separating the two  
99 types of coastlines when assessing tsunami damage (Suppasri et al., 2013; Tsuji et al., 2014; De Risi et al., 2017). This study  
100 focuses on ports located in coastal plains, due to the (i) difficulty of accounting for complexity of flow processes in ria coasts  
101 as well as (ii) significantly less port activity found in the narrow strips of ria coasts. Affected ports, namely Hachinohe, Kuji,  
102 Ishinomaki, Sendai, Soma and Onahama, located in coastal plains were selected as study sites for our damage assessment (Fig.  
103 1).  
104



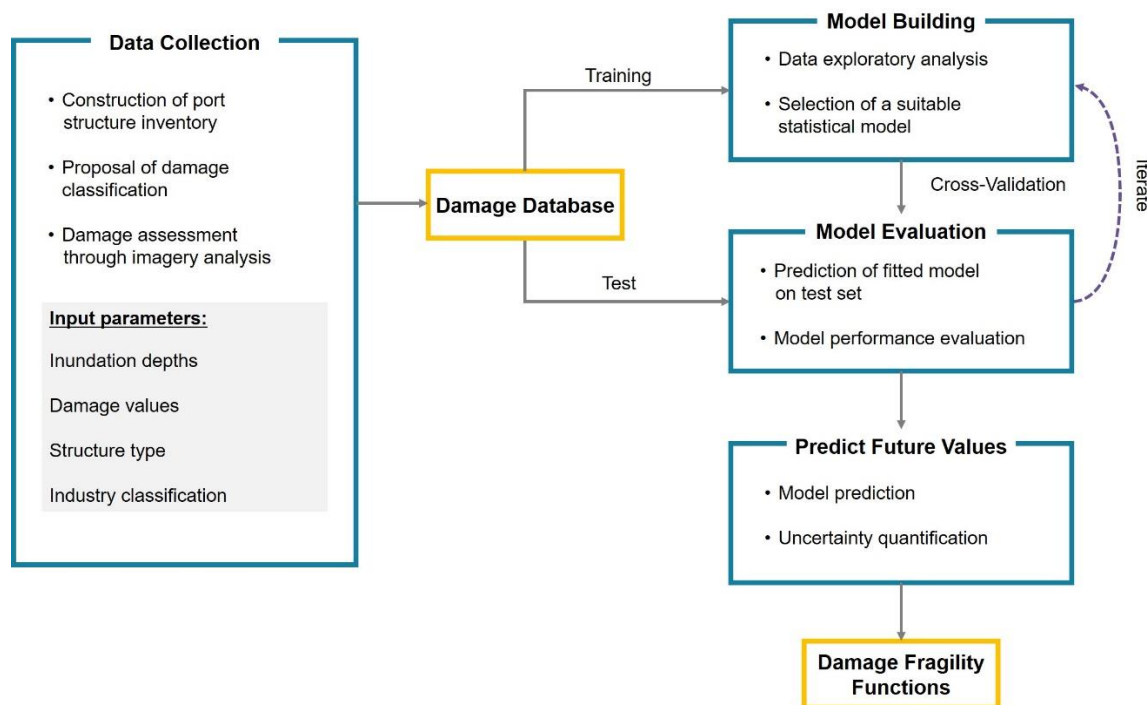
105  
106 **Fig. 1.** Six of the affected ports (circled dots) were selected in this study due to similarities in their coastal morphologies –  
107 they are located in coastal plains. Tsunami inundation heights were measured and collected by the Tohoku Tsunami Joint  
108 Survey (TTJS, 2011) team. Inundation heights refer to the maximum height of tsunami inundation above the mean sea level  
109 in Tokyo Bay (the Tokyo Peil datum). The generalized 2011 fault-rupture area (in light blue) was inferred from GPS data  
110 adapted from Ozawa et al. (2011).



### 111 3. Workflow and data sources

112 A goal of this study was to produce tsunami damage fragility functions for industries commonly found in ports and their  
113 hinterlands, such as chemical and energy-related industries. The components required to derive fragility functions include the  
114 explanatory variable (hazard intensity measure), response variable (damage data) and a statistical linking model (Charvet et  
115 al., 2017). At present, a consolidated data source for tsunami damage to port structures has yet to exist. This data gap presents  
116 us with an opportunity to develop a damage database for port structures, and to use the damage data for the construction of  
117 fragility functions. We developed a framework (Fig. 2) for collecting and processing damage data within a database and using  
118 a machine learning workflow to evaluate those data and provide robust fragility functions; more details on our approaches are  
119 provided over the following subsections. We used freely available data where possible to illustrate how our methods can also  
120 be reproduced in other locations. A synopsis of the data used in this study and their sources are presented in Table 1.

121



122

123 **Fig. 2.** The framework of this study follows the approach of a machine learning workflow. A damage database for port  
124 structures is constructed through data collection and processing. The consolidated data is then randomly split into training and  
125 test sets for model building and evaluation. This process is usually iterated until a satisfactory model is selected for the  
126 development of fragility functions. This is usually the case where there are more than one model or parameter to choose from,  
127 whereas in our case, only inundation depth was considered as an explanatory variable.

128



129 **Table 1.** Data used in this study, their sources and the reference period from which data are taken.

Data	Source	Data observation/ acquisition period	Citation
Tsunami inundation depths	Ministry of Land, Infrastructure, Transportation and Tourism (MLIT)	Mar 2011 – Dec 2012	Ministry of Land, Infrastructure, Transportation and Tourism (2014)
Building database	Ministry of Land, Infrastructure, Transportation and Tourism (MLIT)	Mar 2011 – Dec 2012	Ministry of Land, Infrastructure, Transportation and Tourism (2014)
Port structure footprint for digitisation	GSI Interactive Web: Map/Aerial Photo Browsing Service;	-	Geospatial Information Authority of Japan (2013)
	Google Earth engine	Mar 2009 – Sep 2010	© Google Earth 2020
Aerial images for damage assessment	Google Earth engine;	Mar 2009 – Sep 2010 + Mar 2011 – May 2011 ++ Feb 2012 +++	© Google Earth 2020
	GSI Map: Aerial Photo of Affected Area	Mar 2011 – May 2011 ++ Apr 2012 +++	Geospatial Information Authority of Japan (2012a)
Oblique images for damage assessment	GSI Map: Oblique Photo of Affected Area	May 2011 ++	Geospatial Information Authority of Japan (2012b)
Street view images for damage assessment	Google Street View	Jul 2011 – Aug 2011 ++ Aug 2013 +++	© Google Street View 2020
Landuse (industry) classification	Google Maps	-	© Google Maps 2020

+Pre-tsunami, ++Immediate phase after tsunami and +++One to two years after tsunami (Intermediate phase) for damage assessment



## 131 **4. Data collection**

### 132 **4.1 Establishing a damage database**

133 The port structures referred to in this study collectively consist of a mixture of buildings and industry-related non-building  
134 structures (henceforth referred to as port infrastructure). Detailed building damage data have been collected by Ministry of  
135 Land, Infrastructure, Transportation and Tourism (MLIT, 2014) post-tsunami. However, the MLIT database predominantly  
136 consists of residential, commercial and some industrial buildings. Buildings within the port area are mostly missing from the  
137 database, and infrastructure such as silos, cranes and towers were not identified in the MLIT database.

138 To develop our own database of port structures, we extended the MLIT database, which already consisted of outlines of 3,057  
139 buildings. To build the new database, port structure outlines ( $n = 2,173$ ) were digitised into a Geographic Information System  
140 (ArcMap 10.5) using building footprints from the Geospatial Information Authority of Japan Interactive Map platform (GSI,  
141 2013) as well as pre-tsunami aerial images from Google Earth Engine (Table 1). We identified 3,343 buildings and 1,887  
142 infrastructure (5,230 total). The database is stored in the form of a Geographic Information System (GIS) attribute table. For  
143 each structure, we collected information on

- 144 (1) the type of industry
- 145 (2) the name of port
- 146 (3) the name of company at the time of tsunami (where available)
- 147 (4) maximum inundation depth values
- 148 (5) assigned damage state and,
- 149 (6) structure type (building or infrastructure)

### 150 **4.2 Attributes of port structures and industry**

151 Unique to this work, damaged structures were classified according to their industry type (Table 2). As with the construction  
152 of any fragility function, a key assumption is that structures under the same taxonomy are likely to perform similarly when  
153 exposed to a given hazard intensity (Pitilakis et al., 2014). For that reason, the classification of structures determines the  
154 robustness of the fragility functions developed. It was therefore important to create a suitable taxonomy for the types of  
155 structures being studied. Conventionally, building damage has been assessed by separating the buildings into their various  
156 construction types (e.g. masonry, wood, steel, unreinforced and reinforced concrete). Charvet et al. (2014) noted differences  
157 in the performance of buildings with different construction types to tsunami impacts following the Tohoku event. However,  
158 port structures consist of both buildings and infrastructure, with the infrastructure of a highly specialised nature where the  
159 design and construction criteria are industry-specific. A more suitable approach then would be to classify port structures  
160 according to their industry.



161 Different types of port activities occupy the port area. Aside from the core business of terminal operations, the port is also host  
162 to distribution centres and non-maritime activities. To the best of our knowledge, there is no standard industrial classification  
163 for port activities. We therefore proposed a broad classification for the port activities found in Tohoku ports, according to the  
164 general industry that they fall into (Table 2). Classification for non-maritime port industries was adapted from the terminologies  
165 used by European Sea Ports Organisation (ESPO, 2016) for the various industrial sectors found in European ports. We used  
166 Google Maps and Google Street View to identify the business nature of each company (industry type), commonly through the  
167 name of the company at the time of the tsunami. We identified eight main port industries based on our proposed taxonomy.

168

169 **Table 2.** Proposed classification for port activities found in the Tohoku region.

	<b>Industry type</b>	<b>Description of port activities</b>
Maritime industries	Cargo handling industry	Cargo handling services such as loading and unloading of ships (stevedoring) as well as the handling of cargo on shore.
	Warehousing and distribution	Cold storage, warehousing and logistics support.
Non-maritime port-related industries	Chemical industry	Bulk chemical production e.g. alkane, propane and fertilisers.
	Construction materials industry	Concrete and cement manufacturing. Asphalt and wood processing.
	Energy-related industry	Coal power generation. Electric power generation and distribution.
	Food industry	Seafood processing and food packaging. Feed manufacturing.
	Manufacturing industry	Metal and alloy products. Plywood and paper products.
	Petrochemical industry	Oil depots, reserves and refineries.

170

### 171 **4.3 Maximum inundation depths**

172 Various tsunami hazard intensity measures (e.g. inundation depth, flow velocity and force) have been used in literature to  
173 estimate structural fragility to tsunami impacts. Past studies (Macabaug et al., 2016; Park et al., 2017; Attary et al., 2019) have  
174 shown that no single measure can fully characterise structural fragility to tsunami impacts as it is impossible to explain a  
175 complex phenomenon through a sole parameter. For the purpose of this study, observed maximum inundation depth was  
176 chosen as the representative intensity measure manifesting damage since depth is more easily estimated from field survey after  
177 tsunami events as compared to other flow values, which typically have to be simulated. Using observational data also  
178 minimises the uncertainty in intensity measure as compared to using simulated data (e.g. velocity and force).





179 Inundation characteristics were recorded and collected from a number of sources, namely tsunami trace heights by the Tohoku  
180 Tsunami Joint Survey Group (TTJS, 2011), MLIT survey, photographs, videos, eyewitness accounts and other reports  
181 (Leelawatt et al., 2014). The MLIT (2014) compiled all the maximum inundation depth values and building data into a single  
182 database. Inundation depth refers to the depth of floodwater above ground. Each building surveyed in the MLIT database is  
183 pegged with maximum inundation depth values, and where values were not available for some buildings (e.g. those that were  
184 washed away), they were interpolated from nearby buildings with inundation depth values (De Risi et al., 2017). Similarly, for  
185 buildings and infrastructure that were identified in this study, we interpolated inundation depth values from neighbouring  
186 surveyed buildings.

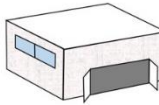
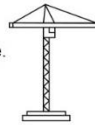
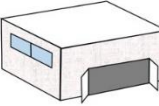

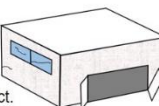

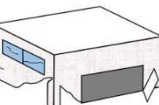

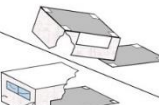
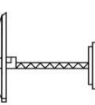
#### 187 **4.4 Proposed damage classification scheme**

188 For the first time, a damage classification scheme for tsunami damage to port structures is being proposed (Fig. 3). The MLIT  
189 adopted a damage classification scheme for building damage assessment following the 2011 Tohoku tsunami (see Leelawatt  
190 et al., 2014). Naturally, subsequent studies that used the MLIT damage database to analyse damage and derive fragility  
191 functions followed the same classification scheme. The pitfalls of adopting the MLIT damage classification have been  
192 highlighted in several studies (Leelawat et al., 2014; Charvet et al., 2015; Charvet et al., 2017). Firstly, the MLIT classification  
193 consists of six damage states, which were found to have overlaps in their definitions (Leelawat et al., 2014; Charvet et al.,  
194 2015). The overlapping definitions might have resulted in buildings being wrongly classified when performing damage  
195 assessment. Ideally, damage states should be presented in a mutually exclusive and consecutive order (Charvet et al., 2015).  
196 Secondly, descriptions in the MLIT classification scheme do not distinguish between structural and non-structural damage.  
197 Therefore, the structural response of the buildings assessed is not being explicitly assessed. Additionally, by specifying the  
198 range of inundation depths associated with each damage state, such definitions allude to inundation depths being a condition  
199 of damage. This contradicts the objective of developing fragility functions as predictive models of damage. Over and above  
200 the limitations outlined, the MLIT damage classification solely describes damage to buildings, which is otherwise unsuitable  
201 for port structures.

202 To address the limitations of the existing damage classification of MLIT, we proposed a new damage classification for port  
203 structures. This new classification scheme provides damage descriptions for both buildings and infrastructure. Degrees of  
204 damage are classified into four levels (with damage state DS 0 being no damage), ensuring that the descriptions for each  
205 damage state are mutually exclusive and in increasing order. Descriptions also include the expected serviceability of the  
206 structure at each damage state. Pitalakis et al. (2014) argued that physical damages would reflect the expected serviceability  
207 of the structure (condition for use) and its corresponding functionality (i.e. can its functions still be fulfilled?). The structural  
208 integrity of port structures is also being considered. For instance, between DS 2 and DS 3, damage is distinguished by whether  
209 it only affected non-structural components and/or roof (DS 2), or structural components such as columns and beams (DS 3).  
210 We assumed that when the structural integrity of a structure is compromised, the structure would be removed.

211



Damage State	Damage Description	
	Buildings (B)	Infrastructure (I)
DS 0	<ul style="list-style-type: none"> <li>Little to no water penetration.</li> <li>Non-structural components (windows and door) and roof remain intact.</li> </ul> 	<ul style="list-style-type: none"> <li>No floodwater impacts on infrastructure.</li> </ul> 
	<i>Serviceability:</i> Ready for immediate use	
DS 1	<ul style="list-style-type: none"> <li>Water penetration.</li> <li>Non-structural components and roof remain intact.</li> </ul> 	<ul style="list-style-type: none"> <li>No visible damage from outside of infrastructure.</li> </ul> 
	<i>Serviceability:</i> Ready for immediate use but requires interior restoration, such as drying of floors and walls, repainting, repairs to plumbing and electric systems.	
DS 2	<ul style="list-style-type: none"> <li>Non-structural components and/or roof have sustained damage.</li> <li>Structural components are intact.</li> </ul> 	<ul style="list-style-type: none"> <li>Some damage to infrastructure, while foundation or base remains intact.</li> </ul> 
	<i>Serviceability:</i> Obvious repair works in the intermediate period after the tsunami. Operational only after repairs.	
DS 3	<ul style="list-style-type: none"> <li>Structural components (columns and beams) have sustained damage, or rackings have buckled and folded.</li> </ul> 	<ul style="list-style-type: none"> <li>Foundation or base of infrastructure has folded or buckled.</li> </ul> 
	<i>Serviceability:</i> Not repairable. Replacement or removal of building in the intermediate period after the tsunami.	
DS 4	<ul style="list-style-type: none"> <li>Total structural failure.</li> <li>Building has either overturned or slid from original position.</li> </ul> 	<ul style="list-style-type: none"> <li>Infrastructure has overturned or slid from original position.</li> </ul> 
	<i>Serviceability:</i> Not operational.	

212  
 213 **Fig. 3.** Proposed new damage classification for port industries. Descriptions for damage to both buildings and non-building  
 214 infrastructure are provided in the classification table. DS 1 and DS 2 are considered as non-structural damages, while DS 3  
 215 and DS 4 are structural damages.

216 **4.5 Damage assessment through spatio-temporal analysis**

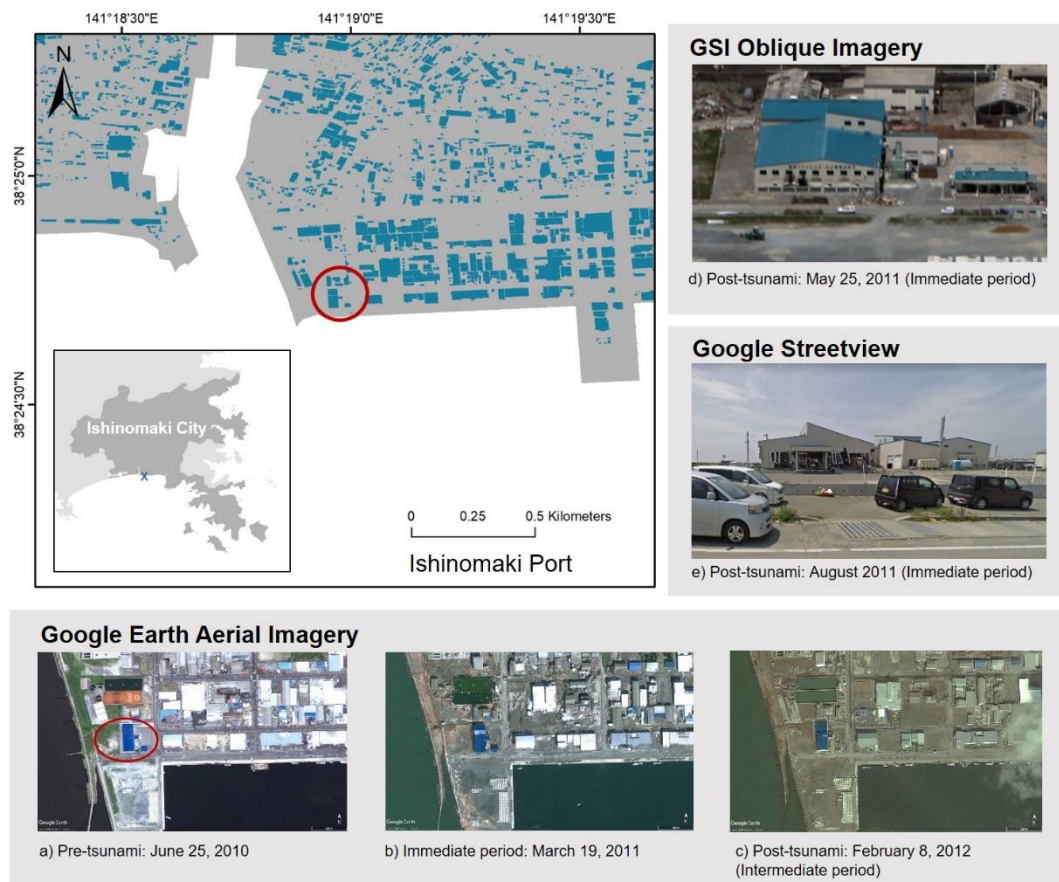
217 A combination of free-to-use sources were used to inform our classification decisions when assigning damage states to  
 218 individual port structures (Table 1). Port structures were assessed through the analysis of satellite imagery, using pre- and post-  
 219 tsunami images from Google Earth engine and Geospatial Information Authority (2012a), as well as photographic  
 220 interpretations of post-tsunami oblique images from Geospatial Information Authority (2012b). Pre- and post-tsunami images  
 221 refer to observations made before 11 March 2011, and on and after 11 March 2011 respectively (Table 1). Apart from aerial



222 and oblique images, we visually assessed the conditions of port structures through Google Street View images. Google Street  
223 View, a service available on Google Maps web, provides panoramic view of the landscape at a street level. An example of  
224 how a building or infrastructure was being assessed is illustrated in Fig. 4.

225 The three types of images (aerial, oblique and street view) provided different, yet complimentary, types of information. Aerial  
226 images were particularly useful in assessing washed away and collapsed structures (DS 4). Street View images were used to  
227 identify damage from façade level, which supplemented as “ground truth surveys”. The high-resolution imagery provided by  
228 Google Street View allowed us to pick up finer details such as structural and non-structural damage to port structures, which  
229 would otherwise be missing from aerial imagery. However, because Street View imagery was captured through vehicle-  
230 mounted cameras, the availability of these images are constrained by the accessibility of roads by the vehicle at the time of  
231 survey. Where imagery was not captured by Google Street View due to such constraints, we capitalised on the alternative  
232 views provided by GSI oblique images.

233 Advances in mapping technologies mean that temporal changes are also being captured and documented in these mapping  
234 applications. The time-slider functions on Google Earth engine and Google Street View web, as well as the date stamps on  
235 GSI images, allowed us to review temporal changes in the built environment. For images in Google Earth and Google Street  
236 View, different phases of the tsunami, i.e. pre-tsunami (before March 2011), immediately after the tsunami (up to 6 months  
237 after the tsunami) and the intermediate recovery phase (1 – 2 years), were all captured in the same point locations. With  
238 coordinates being embedded in the aforementioned data sources, we were also able to reference GSI aerial and oblique post-  
239 tsunami images to the same locations. The large amount of high-quality data provided by these image databases and mapping  
240 applications have been a large driver of our data collection in this study.





## 253 5.1 Evaluation of statistical models available

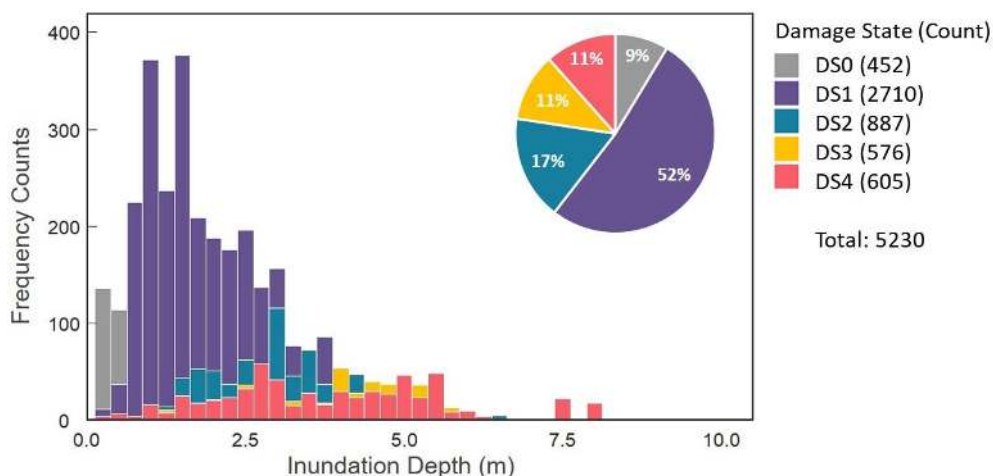
254 In recent years, a number of studies evaluated the suitability of various statistical models in representing tsunami damage to  
255 structures (Charvet et al., 2014; Macabaug et al., 2016; Charvet et al., 2017). Parametric (e.g. Ordinary Least Square regression,  
256 Generalised Linear Model or ordinal logistic regression models), semi-parametric (e.g. Generalised Additive Model) and non-  
257 parametric (e.g. Kernel Smoother) statistical model types are amongst the most commonly used. These statistical models are  
258 extensively reviewed in Rosetto et al. (2014), Lallemand et al. (2015), Macabaug et al. (2016) and Charvet et al. (2017), and  
259 readers are referred to these studies for a more comprehensive understanding of the advantages and disadvantages of using the  
260 various types of statistical models.

261 Generalised Linear Models (GLM), an extension of classical linear regression models, have been recommended as more  
262 reliable forms of fragility functions for the following reasons:

- 263 • Discrete probability distributions can be used to predict discrete responses (Charvet et al., 2017). This is especially  
264 important for categorical data (such as damage states), because it is statistically incorrect to assume that the difference  
265 between categories is linear/continuous, e.g. the difference between DS 1 and DS 2 holds the same meaning for the  
266 difference between DS 2 and DS 3 (Guisan and Harrell, 2000).
- 267 • Unlike classical linear regression models (e.g. ordinary least square regression) which assume either a normal or  
268 lognormal distribution, the response variable need not be normally distributed and can take on any of the exponential  
269 family distributions.
- 270 • It does not assume a linear relationship between the explanatory variable and response variable, but a linear  
271 relationship is assumed between the transformed response through a link function and the explanatory variables.
- 272 • Maximum likelihood estimation (MLE) is used rather than ordinary least squares to estimate the parameters. MLE  
273 has the advantage of explicitly reflecting the probability distribution of the random variable of interest.
- 274 • Overfitting of data can be avoided by using cross-validation analysis to determine optimal model parameter values.
- 275 • Model uncertainty can be quantified by supplementing the median of the response with confidence or prediction  
276 intervals.

## 277 5.2 Data exploratory analysis

278 The response variable is ordinal (in the sense that  $DS\ 0 < DS\ 1 < DS\ 2 < DS\ 3 < DS\ 4$ ). A visual inspection of the distribution  
279 of depth given damage data (Fig. 5) indicates non-normality, with the distribution skewed towards the right, indicating a  
280 lognormal transformation of inundation depth variable would be appropriate. Frequency counts of the damage data show that  
281 damage state (DS 1) makes up the majority of the dataset ( $n = 2710$ ), and DS 3 and 4 a much smaller proportion ( $n = 576$  and  
282  $n = 605$  respectively).



283

284 **Fig. 5.** Histograms of each damage state. Distribution of damage data indicates non-normality and DS 1 accounts for the  
285 majority of the dataset. Outliers exist in DS 3 and 4, with no damage states recorded for inundation values between 6 to 7.4  
286 metres. Outliers are not removed from the model, as they are legitimate observations and possible outcomes.

### 287 5.3 Selection of a suitable statistical model

288 An ordinal logistic regression model, an ordinal and logistic recourse of GLMs, is adopted. It has the additional advantage of  
289 accounting for and maintaining the ordered nature of damage-state data. As this model recognises the ordered nature of the  
290 damage states, overlapping pathways of the fragility functions can be avoided (Charvet et al., 2017). Overlapping fragility  
291 functions, as is common when fitting separate GLMs, may unwittingly imply that the probability of a higher damage state (e.g.  
292 DS 4) being exceeded is higher than that of a lower damage state (e.g. DS 3) as inundation depth increases. Ordinal models  
293 also make full use of the ranked data rather than simplifying it into binary exceedance and non-exceedance, and therefore  
294 preventing the loss of information (Ananth and Kleinbaum, 1997).

295 The dependence of the response variable DS on predictor variable X can then be represented as follows

296

$$P_{DS} = P(ds \geq DS_i | X_j)$$

297 , where  $DS_i$  refers to the  $i_{th}$  damage state,  $j$  the specified predictor (IM) or combination of predictors. The model relates the  
298 probability of the outcome,  $P_{DS}$ , to all explanatory variables ( $X_1, X_2, \dots, X_j$ ) through a linear predictor. There are three basic  
299 components to any GLM, and Table 3 describes the components in the context of the ordinal logistic model used in this study.

300



301 **Table 3.** Components of an ordinal logistic regression model

Random Component	<i>The probability distribution of the response variable.</i>
	A multinomial distribution is assumed for the cumulative probabilities in an ordinal logistic regression model.
Systematic Component	<i>The explanatory variable (<math>X_j</math>) or the linear combination of the explanatory variables (<math>X_1, X_2, \dots, X_j</math>) in creating the linear predictor e.g. <math>\beta_0 + \beta_1 X_1, \beta_2 X_2 + \dots + \beta_j X_j</math>, where <math>\beta_0</math> and <math>\beta_{1,j}</math> are transformed constant and regression coefficients through maximum likelihood estimation.</i>
Link function	<i>The link between random and systematic components.</i>

Describes how the cumulative probability  $P_{DS_i}$  of the expected outcome for any damage state  $DS_i$  relates to the linear predictor of explanatory variables  $X_j$ . In this instance, the link function chosen takes on a logit form  $g$  where

$$g(P_{DS_i}) = \log\left(\frac{P_{DS_i}}{1 - P_{DS_i}}\right)$$

, with

$$P_{DS_i} = P(ds \geq DS_i | X_j) \quad \forall i \in (1, \dots, I)$$

Therefore, the dependence of the response variable DS on the linear predictor can be re-expressed as

$$\log\left(\frac{P_{DS_i}}{1 - P_{DS_i}}\right) = \beta_{0,i} + \beta_1 X_1 + \beta_2 X_2 + \dots + \beta_j X_j$$

$$\log\left(\frac{P_{DS_i}}{1 - P_{DS_i}}\right) = \beta_{0,i} + \sum_{j=1}^J \beta_j X_j$$

The corresponding regression coefficients  $\beta_{1,j}$  in the link function are fixed across every damage state except for the intercept, so as to maintain the order of the response categories.



303 The conditional probability  $P(ds \geq DS_i | X_j)$  is a common vector of regression coefficients  $\beta$ , which connects probabilities for  
304 varying levels of damage. When expressing the cumulative probabilities of each damage state as separate curves, the  
305 relationships between damage states in increasing order of severity are defined as follows:

$$306 \quad P_{DS} = P(ds = DS_i | IM = X_j) = \begin{cases} 1 - P(ds \geq DS_i | X_j) & i = 0 \\ P(ds \geq DS_i | X_j) - P(ds \geq DS_{i+1} | X_j) & 0 \leq i \leq N_{DS} \\ P(ds \geq DS_i | X_j) & i = N_{DS} \end{cases}$$

307  
308 , where  $N_{DS}$  refers to the number of damage states, including DS 0 (Macabaug et al., 2016).

## 309 6. Model evaluation

### 310 6.1. 10-fold cross-validation

311 Model accuracy was used as a quantitative indicator of the performance of our models. We wanted to assess the goodness-of-  
312 fit of the models and determine its predictive ability. It was difficult to test the predictive ability of our models where there  
313 were no further samples to test with. In order to optimise model design while preventing overfitting, the cross-validation  
314 method was applied to evaluate the prediction accuracy of our models. Cross-validation techniques make use of the available  
315 dataset by dividing them into two subsamples – one to train the model and the other to predict the model on.

316 One cross-validation technique is K-fold, where the dataset is divided into K number of approximately equal-sized subsets as  
317 illustrated in Fig. 6a. One subset is taken out as a test set for validation, and the remaining  $K - 1$  subsets are then used to train  
318 a model. This hold-out method is then repeated for K number of times, with a new subset being used as a test set in each  
319 iteration. Only after all K models are fitted, statistics of the model performance are tabulated. For the purpose of this study, a  
320 10-fold cross-validation approach was taken.

321 The accuracy of a model is determined by the proportion of correctly classified responses. When applied to the k-fold  
322 technique, the fitted model is used to predict response on the held-out  $k^{\text{th}}$  subset in each iteration. The recorded response is  
323 tabulated against actual observations in the  $k^{\text{th}}$  subset and a confusion matrix is constructed as demonstrated in Fig. 6b. The  
324 diagonal of the confusion matrix represents the sum of correctly predicted response, the proportion of correctly classified  
325 response is then calculated by

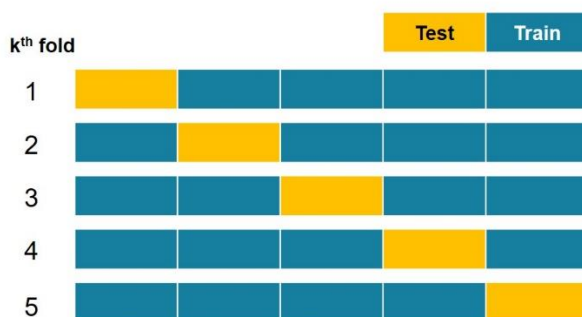
$$326 \quad Accuracy = \frac{\text{Sum of correctly predicted response}}{\text{Sum of total observations}}$$

327  
328 Accuracies are recorded in each iteration of the K-fold, and the mean and standard-deviation of the tabulated accuracies are  
329 taken to assess the predictive ability of the model. All statistical analyses and modelling in this study were carried out using  
330 the statistical software R (R Core Team, 2020).





### a) K-fold cross-validation



### b) Confusion matrix for accuracy

		Predicted			
		DS 1	DS 2	DS 3	DS 4
Actual	DS 1	30			
	DS 2		20		
	DS 3			8	
	DS 4				9

Example of  $k^{\text{th}}$  in K number of folds

331

332 **Fig. 6.** (a) An example of a 5-fold cross-validation technique for the purpose of illustration. The same dataset can be folded  
 333 into 5 equal sizes, and one fold is held-out for testing and the remaining 4 folds are used to develop a training model to predict  
 334 the accuracy of the training model. This is repeated 5 times, with accuracies being tabulated in each iteration. (b) Accuracy  
 335 table (confusion matrix) is produced in each iteration of the k-folds. The sum of the diagonal in the table is divided by the sum  
 336 of observations to get the percentage of accuracy in the  $k^{\text{th}}$  fold.

## 337 6.2 Quantification of uncertainty

338 The fragility functions, when presented as curves or plots, represent the expected value of the response variable. Therefore,  
 339 they represent only a sample estimate of the population values. Statistical variations of the fragility functions can be accounted  
 340 for by estimating the confidence intervals. In this study, we adopted bootstrap-based confidence intervals to estimate the  
 341 uncertainty in estimation or prediction. The bootstrap method treats the original dataset of values as a realised sample from the  
 342 true population and does not make any assumptions about the underlying distribution of the population parameters (Yung and  
 343 Bentler, 1996). Values from the original dataset are resampled repeatedly, with replacement. This was done for 1000 iterations,  
 344 with the predicted logit computed in each iteration. To derive a 95% confidence band, the 2.5<sup>th</sup> and 97.5<sup>th</sup> quantiles of the 1000  
 345 estimates were drawn at each inundation depth interval (0.01m).

## 346 7. Results

### 347 7.1. Damage database for port structures

348 To characterise the vulnerability of assets in various port industries, damage assessment was performed for buildings and  
 349 infrastructure in the Tohoku region. We compiled damage information on port structures into a database, which is available  
 350 online through an unrestricted data repository (DR-NTU) hosted by Nanyang Technological University  
 351 (<https://doi.org/10.21979/N9/OTZMT1>) (Chua et al., 2020).

352 The port damage database consists of 5,230 port structures, of which 3,343 are buildings and 1887 are infrastructure. The port  
 353 structures were identified in six case study ports, across eight port industries. The damage dataset show that most port structures

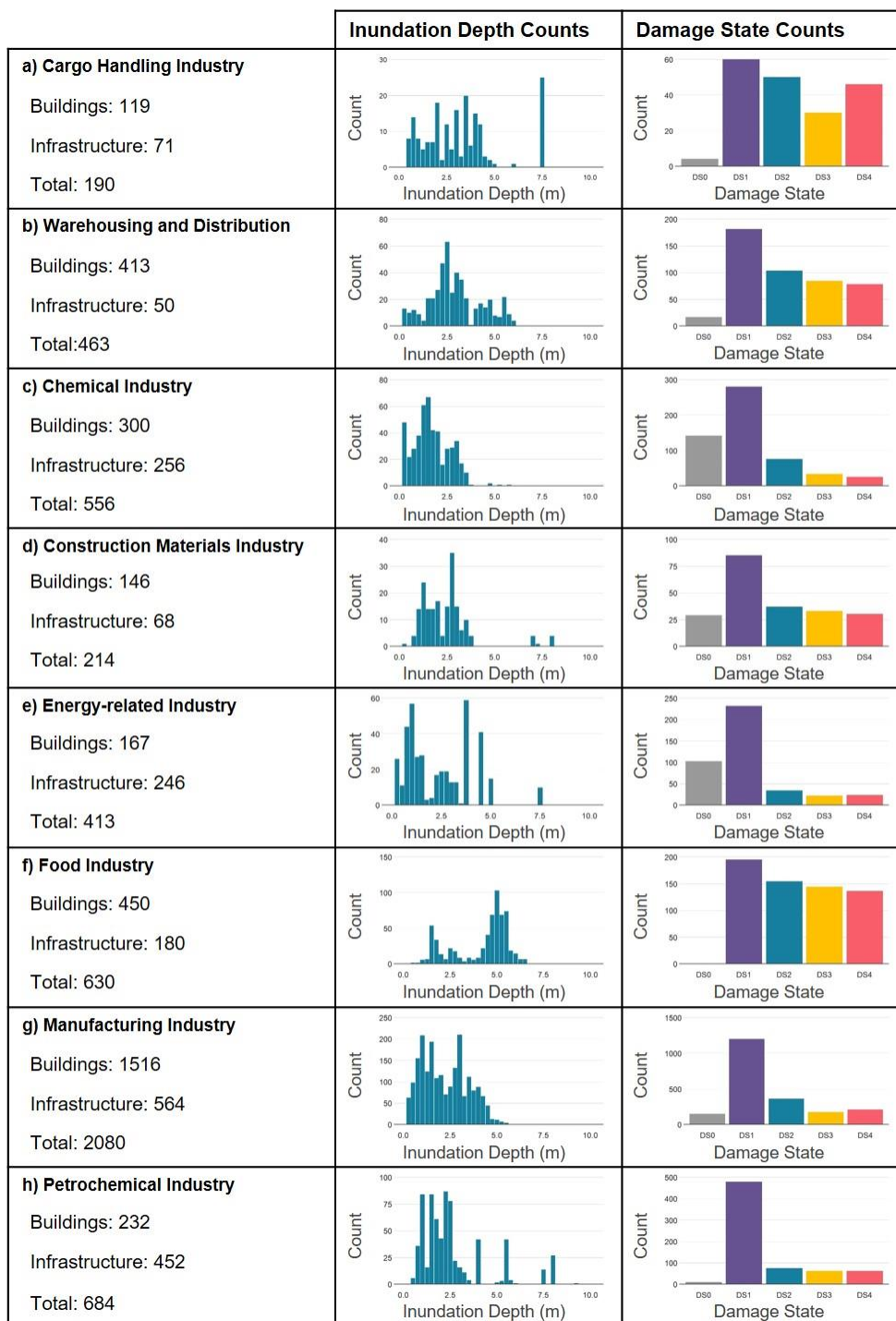


354 sustained minimal structural damage classified as damage state DS 1 (Table 4). Consistently for all port industries, the majority  
 355 of the observed damage corresponds to DS 1 (Fig. 7.) Notably, many industries such as chemical, petrochemical and energy-  
 356 related industries sustained minimal structural damage mainly due to flooding at DS 1, which only required some clean up and  
 357 interior restoration and remained mostly operational after restoration. On the other hand, cargo handling and food industries  
 358 sustained a wide range of damage from minimal damage (DS 1) to total damage (DS 4), corresponding to nearly all damage  
 359 states. Tsunami floodwaters at depths of less than 5 metres inundated most port structures. In extreme cases, inundation depths  
 360 affecting port structures reached as high as 7.5 metres. The minimum recorded inundation depth was 0.1 m.

361

362 **Table 4.** Summary of port structures identified in the various ports, sorted according to their industries.

	North Tohoku		South Tohoku				Total
	Hachinohe	Kuji	Ishinomaki	Sendai	Soma	Onahama	
Cargo Handling Industry	31	9	31	32	25	62	190
Warehousing and Distribution	111	16	175	105	39	17	463
Chemical Industry	236	-	208	27	85	-	556
Construction Materials Industry	29	20	20	99	9	37	214
Energy-related Industry	125	-	-	104	134	50	413
Food Industry	12	37	430	151	-	-	630
Manufacturing Industry	1010	60	587	279	144	-	2080
Petrochemical Industry	202	41	38	324	-	79	684
<b>Total</b>							5230



363  
 364 **Fig. 7.** Data attributes of the port industries affected by the 2011 Great East Japan tsunami.



## 365 7.2 Damage fragility functions for port industries

366 Damage fragility functions were produced for eight major port industries as depicted in Fig. 8. Individual fragility curves were  
367 plotted for each damage state and the solid lines represent the probabilities of a structure exceeding each damage state given a  
368 range of inundation depths and the shaded regions their corresponding 95% confidence intervals.

369 The fragility functions (Fig. 8) suggest that chemical, cargo handling, and construction materials industries are more  
370 vulnerable. Higher probabilities of damage exceedance are reached at a more rapid rate as compared to other industries. In  
371 contrast, energy-related industry and warehousing and distribution are showing a gentler incline in damage probability for  
372 higher levels of damage (DS 3 and DS 4), indicating a greater resistance to tsunami impacts. A key assumption of fragility  
373 studies and of this study is that damage is directly related to the properties of the elements at risk. Thus, aside from tsunami  
374 intensity measures, the composition and structural design of each industry could determine the differences in vulnerabilities.  
375 For example, power plants (energy-related industries) and warehouses are structurally robust by design. Most heavy equipment  
376 found in power plants is normally supported in large reinforced concrete foundations or housed in large steel structure buildings  
377 (Cruz and Valdivia, 2011) and is therefore more resistant to tsunami loads. Likewise, many warehouses in the studied ports  
378 were reinforced concrete buildings with their warehouse floor raised above road levels, which increased the height of non-  
379 structural elements (e.g. docks and doors) relative to tsunami inundation. Comparatively, chemical facilities typically consist  
380 of more fragile components which are not part of the primary load resisting systems such as pipelines, pumps, compressors  
381 and tanks, and they are extremely vulnerable to damage from tsunami inundation and forces. As observed in the 2011 event,  
382 hydrodynamic and hydrostatic forces from the tsunami resulted in the breaking of pipe connections, floating tanks and  
383 overturning of unanchored infrastructure (Krausmann and Cruz, 2013). Meanwhile in cargo handling facilities, loading and  
384 unloading infrastructure was mostly anchored, but instances of cracked pavements and damaged crane rail foundations by the  
385 earthquake and tsunami were reported to result in the derailment and collapse of cranes (Technical Council on Lifeline  
386 Earthquake Engineering, 2017). Nonetheless, other factors such as debris impact and proximity to shoreline should not be  
387 discounted when considering the differences in the response of each industry to tsunami impacts.

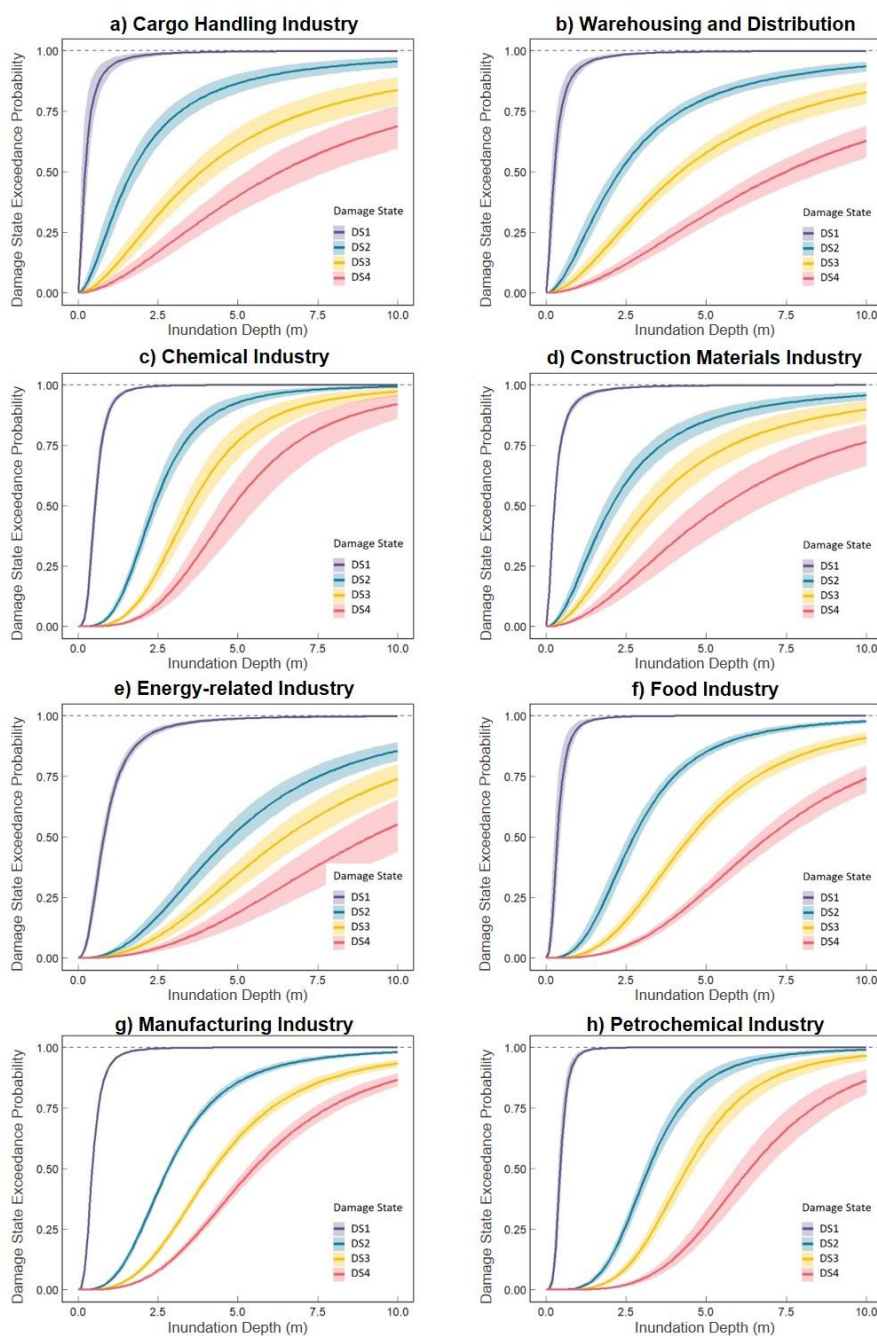
388 For each damage state, we considered the minimum depths where damage exceedance probability reaches near 1 or becomes  
389 nearly certain. Minimum damage (DS 1) is almost certain at 2.5 m consistently for all industries except energy-related industry.  
390 DS 1 occurs when there is water penetration into the building and interior restoration is required (Fig. 3). Logically, water  
391 penetration into buildings would be expected from 0.45 m since buildings are required to be constructed 0.45 m above road  
392 level as specified by the Building Standard Law of Japan (Building Centre of Japan, 2013). Threshold depths for DS 1 might  
393 have occurred at 2.5 m because of the aggregation of data for both infrastructure and buildings. We observed that there were  
394 many buildings (especially warehouse) and infrastructure such as storage tanks and silos that were elevated above ground and  
395 therefore, the number of exposed assets at lower inundation depths were reduced. The trend for other damage states is however  
396 not obvious and it is difficult to pinpoint minimum depth values where damage becomes certain.



397 A threshold value is said to be reached when damage curves from all states of damage converge at the probability of near  
398 100%. Key threshold value can be defined as the parameter (in this case, inundation depth) criteria at which DS 4 (collapse)  
399 becomes certain. Earlier studies of the 2011 Great East Japan tsunami (Suppasri et al., 2013; Charvet et al., 2014) examined  
400 the key threshold values for buildings, using damage data provided by MLIT. Suppasri et al. (2013) identified 2 m to be the  
401 key threshold value for all building types. More recent analysis found inundation depth thresholds to differ between  
402 construction types: from 2 m for wooden buildings (Charvet et al., 2014) to more than 10 m (Charvet et al., 2015) for steel and  
403 reinforced concrete construction types. Similar patterns have emerged in the present analysis. The near 100% probability of  
404 collapse occur at inundation depth exceeding 10 m for all industries. As such we were unable to quantify the key threshold  
405 values for collapse for port industries. There are several possible reasons for this observation. Two likely explanations stand  
406 out. The first being port structures are structurally much more resistant to tsunami loads than regular low-rise buildings because  
407 industrial buildings and structures are designed to withstand greater loads, including but not limited to dead loads, live loads,  
408 wind and earthquake loads. Therefore, greater tsunami inundation depths are required to overcome the resistance of port  
409 structures. A second possible explanation is that inundation depth alone is insufficient to explain damage, although it provides  
410 a first indication.

411 The effects of uncertainty were quantified through the construction of confidence intervals around the mean of the resulting  
412 probabilities. Confidence intervals around DS 1 are consistently narrow in width for all industries (Fig. 8), which could be  
413 associated with its large sample size. Contrastingly, for higher levels of damage (DS 3 and DS 4), confidence intervals tend to  
414 widen towards higher inundation depths. An observation made in the process of damage data collection through photographic  
415 interpretations was that many structures sustained very little damage despite high inundation depth values, which explains the  
416 smaller sample sizes and therefore wider confidence intervals for DS 3 and DS 4 at higher depth values. In the same way,  
417 industries with the widest confidence intervals such as cargo handling industry and construction materials industry tend to  
418 have smaller sample sizes. By contrast, variabilities around the median curves tend to be smaller for the manufacturing  
419 industry, food industry, warehousing and distribution and petrochemical industry due to their larger sample sizes.

420



421

422 **Fig. 8.** Fragility curves with 95% confidence bands for port industries identified in this study. Chemical, cargo handling and  
423 construction materials industries appear to be more vulnerable to tsunami inundation depths, while petrochemical and  
424 warehousing and distribution industries have lower damage probabilities for the same inundation depths. Wider confidence  
425 bands imply greater variability in uncertainty and could be results of smaller sample sizes.



## 426 8. Discussion

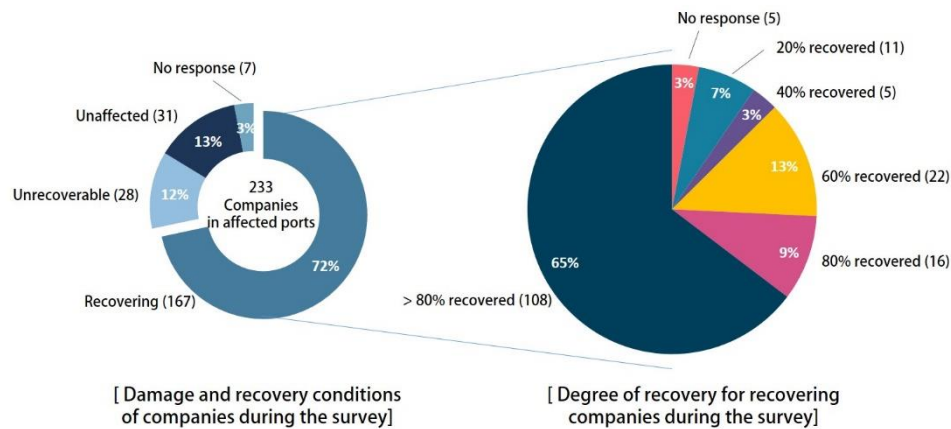
### 427 8.1 Comparison of damage dataset with functionality of port industries post-tsunami

428 We compared the damage database with existing literature to validate our observations. Most of the existing literature are  
429 either limited to descriptive analysis of damage to port facilities or are not available in English. We found only one study to  
430 be comparable with this study, in terms of the quantification of damage to port industries. A post-2011 tsunami survey was  
431 carried out by the Tohoku Regional Development Bureau (MLIT, 2011) between October and November, 2011. We considered  
432 the survey period as the intermediate period for reconstruction after the tsunami. The survey is a questionnaire survey on the  
433 recovery status of companies in tsunami-affected ports, including ports outside of our study sites. 226 of the 233 companies  
434 found in the affected ports responded to the survey. Findings from the survey were adapted from MLIT (2011) and we have  
435 translated them into English (Fig. 9).

436 We drew comparisons between the recovery status of the companies affected (MLIT survey) and the serviceability of port  
437 structures at each damage state (this study). It is difficult to make a direct comparison between the two. While port structures  
438 are the physical components of these companies, port structures and companies are inherently different entities. Therefore, an  
439 assumption made here is that the serviceability of port industries is indicative of the recovery status of the companies surveyed  
440 in the MLIT survey.

441 13% of the companies were found to be unaffected by the tsunami (Fig. 9), which marks a good agreement with our study  
442 where port structures sustaining no damage (DS 0) makes up 9% of the dataset (Fig. 4). In addition, approximately 12% of the  
443 companies found to be unrecoverable, which we assume to correspond to damage state DS 4 (11%) in our study. The MLIT  
444 survey found 72% of the companies to be in various stages of recovery during the survey and a majority (46.8%) of the  
445 companies were almost fully recovered (> 80% recovery) in the intermediate phase. Similarly, a large proportion (52%) of our  
446 damage data falls into DS 1 where port structures can be operational almost immediately after tsunami (Fig. 3). It is  
447 challenging, however, to draw parallel between the degrees of recovery with the damage states presented in this study. We  
448 stress that this approach is a relative measure of the validity of our dataset and damage assessment. Nonetheless, we can infer  
449 that damage observations made from photographic interpretations in this study are rather similar to actual observations.

450



451

452 **Fig. 9.** Damage conditions and degrees of recovery of companies in the tsunami-affected ports of Hachinohe, Kuji, Miyako,  
453 Kaimaishi, Ofunato, Ishinomaki, Sendai-Shiogama, Soma and Onahama. 65% of the recovering companies were almost close  
454 to full recovery (>80%) at the time of the survey. Adapted and translated from MLIT (2011).

## 455 8.2 Fragility models and their classification accuracies

456 Using the 10-fold cross validation technique, we evaluated the prediction accuracies of our models. Mean accuracies and their  
457 standard deviations for each industry are illustrated in Table 5. Port structures have an overall accuracy of 59%. The  
458 petrochemical industry, energy-related industry, chemical industry and manufacturing industry display higher accuracies –  
459 75%, 70%, 69% and 64% respectively. In contrast, warehousing and distribution industry, cargo handling industry and food  
460 industry display lower prediction accuracies – 40%, 38% and 28% respectively.

461 We looked at the underlying nature of our datasets to better understand the differences in accuracies. The petrochemical  
462 industry, energy-related industry, chemical industry and manufacturing industry display higher accuracies and are represented  
463 by large sample sizes (Fig. 7). On the contrary, the cargo handling industry is represented by only 190 data points. However,  
464 because the food industry is represented by a large sample size but seemingly displays very low accuracy, we were unable to  
465 conclude that sample size has an influence on the accuracies of the fragility models. In addition, the three industries  
466 (warehousing and distribution, cargo handling and food industries) which display low accuracies are well represented across  
467 all damage states.

468 The intrinsic differences between industries could have an effect on reducing accuracies. The composition of buildings and  
469 infrastructure differ from industries to industries. For instance, cargo handling industry, which displays lower accuracy,  
470 typically consists of mobile equipment such as cranes and conveyors as well as temporary transitional storage and components  
471 such as chillers and tanks. Damage to transient port structures as such may be reflected in the damage data as part of the overall  
472 assessment and introduce noise to the damage data, thus reducing model accuracy. In addition, the structural design of port  
473 structures may vary between facilities of the same industry. For example, warehouses in the studied ports were mostly  
474 reinforced concrete buildings, but some were made of mixed materials such as reinforced concrete foundations with light metal





475 or masonry walls. Whereas power plants (energy-related industry) and petrochemical industry are consistent in construction  
476 material and more robust by design, which perhaps explain their higher accuracies. Thus, variability between port structures  
477 of the same industries can also impact accuracy if those variables are not accounted for in the models.  
478 Another possible explanation is that many assets might have sustained extensive damage from earthquake activities such as  
479 ground motion and liquefaction prior to the tsunami, as was observed by Kazama and Noda (2012). A preliminary inspection  
480 of the damage dataset indicated a greater representation of data from ports that have experienced stronger ground motion for  
481 the following industries – food, cargo handling and warehousing and distribution (Table 4). On the other hand, industries that  
482 display higher accuracies have a greater data representation from ports that were not as severely affected by ground motion.  
483 The significance of this relationship between the effects of the preceding earthquake and the damage observed is further  
484 investigated in the proceeding section.  
485 For most industries, our models performed better in terms of their classification accuracies as compared to fragility models  
486 developed for buildings using the MLIT damage classification, which were found to have an accuracy of 52% (Leelawat et  
487 al., 2014). As this is the first time tsunami damage is being quantified as a response of inundation depth for port industries, we  
488 have no other models that we could use for comparison.

489

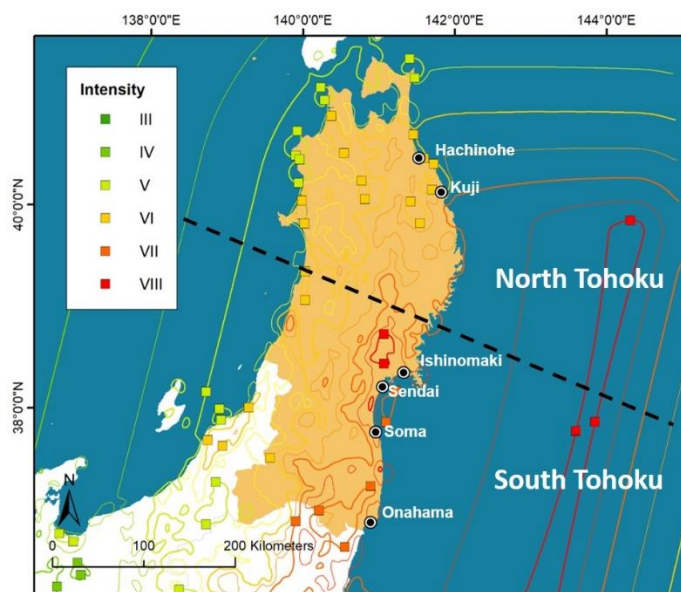
490 **Table 5.** Mean accuracies and standard deviations of accuracies of the various port industries.

Industry Type	Mean Accuracy	SD Accuracy
Cargo Handling Industry	0.374	0.221
Warehousing and Distribution	0.397	0.198
Chemical Industry	0.687	0.300
Construction Materials Industry	0.502	0.285
Energy-related Industry	0.707	0.245
Food Industry	0.283	0.204
Manufacturing Industry	0.638	0.249
Petrochemical Industry	0.746	0.218
All Industries (Whole Tohoku)	0.587	0.203

491



492 **8.3 Effects of pre-tsunami earthquake activities on observed damage to port structures**



493  
494 **Fig. 10.** Mercalli intensities (MI) recorded by United States Geological Survey (USGS, 2020) for the Great East Japan  
495 earthquake and tsunami. Earthquake intensities differ between the northern (MI VI) and southern (MI VII - VIII) regions of  
496 Tohoku. North Tohoku experience less effects from ground shaking than in the South.

497  
498 One of the concerns raised in the process of this research was the effect of ground motion, which preceded the arrival of the  
499 tsunami, on asset damage. The effect of ground motion on damage to coastal structures was studied by Sugano et al. (2014).  
500 The authors noted that in the northern Tohoku region, only little damage was sustained due to ground motion and the damage  
501 observed was to a greater effect due to tsunami inundation. On the other hand, damage due to ground motion was substantially  
502 greater in southern Tohoku region, more specifically coastal areas south of Miyagi Prefecture. Similar observations were made  
503 by Okazaki et al. (2013), whom conducted surveys in Ishinomaki and Sendai ports and found that the two sites were exposed  
504 to both severe ground motions and great tsunami wave heights. Kazama and Noda (2012) have also highlighted the possibilities  
505 of liquefaction prior to the arrival of the tsunami but noted the impossibility of identifying locations of which liquefaction had  
506 occurred after the tsunami.

507 To assess if ground motion-induced damage affects the accuracies of our models, we separated the damage data according to  
508 the locations of ports (between northern Tohoku and southern Tohoku regions). The ports of Hachinohe and Kuji fall within  
509 the northern region, and the ports of Ishinomaki, Sendai, Soma and Onahama are located within the southern region (Fig. 10).  
510 We selected two industries to capture the effect of ground motion, instead of using the entire dataset since it has the effect of  
511 aggregating data from different industries and hence neglect differences in their physical characteristics. The manufacturing  
512 industry was considered because of its high prediction accuracy and its large sample size. The food industry was also

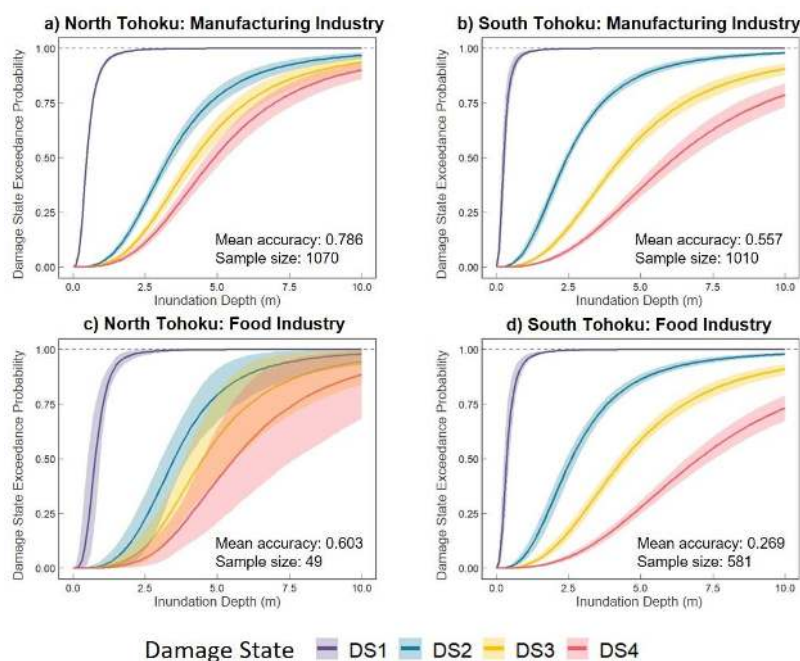


513 considered due to its poor prediction accuracy – we wanted to examine if pre-earthquake activities might explain the poor  
514 prediction ability of the fitted model.

515 Damage data for both industries was split into two sites (North and South Tohoku). For each dataset, an ordinal regression  
516 model was fitted and its response was captured in a 10-fold cross-validation. The resulting fragility models and their mean  
517 accuracies are shown in Fig. 11. We observe that port structures in South Tohoku tend to reach high probabilities of non-  
518 structural (DS 1 and DS 2) damage at lower inundation depths than structures in North Tohoku. This suggests that earthquake  
519 damage might have weakened structures prior to the tsunami, leading to a steeper incline in damage probabilities as compared  
520 to structures in North Tohoku. However, at higher levels of damage (DS 3 and DS 4), ground shaking appears to have had less  
521 influence on damage. For both industries in the northern region, models depict a smaller initial increase in damage for higher  
522 levels of damage DS 3 and DS 4 but probabilities incline more rapidly at higher inundation depths. The opposite holds true for  
523 both industries in the southern region, i.e. damage probability for DS 3 and DS 4 incline at a slower rate at higher inundation  
524 depths implying that a larger depth is required to induce structural damage (DS 3) and collapse (DS 4). Ground shaking  
525 therefore only influenced lower levels of damage, tsunami inundation and flow characteristics still had a greater influence on  
526 higher levels of damage.

527 The mean accuracies of using only datasets from North Tohoku are significantly higher than those of South Tohoku datasets.  
528 It appears that the aggregation of datasets from the two environments has the effect of averaging the mean accuracies for the  
529 whole region (Table 5, Fig. 11). It suggests that damage sustained by port structures in the Southern Tohoku region was  
530 influenced by the compound effects of earthquake and tsunami loads. Inundation depth alone is not sufficient to explain the  
531 damage observed. However, as Charvet et al. (2014) pointed out, it is difficult to distinguish the extent to which buildings had  
532 already been affected by earthquake damage prior to the arrival of the tsunami. Therefore, it was difficult to separate the effects  
533 of ground motion and liquefaction when we developed our fragility models.

534 There are other factors such as debris impact, the effect of shielding and local characteristics of the built environment that may  
535 have influenced the results observed (Tarbotton et al., 2015). Regardless, we note that while the fragility model developed for  
536 food industry using only data from the North has an improved mean accuracy, there is a substantial increase in the uncertainty  
537 of the model (Fig. 11). It is not surprising as wider confidence intervals are a reflection of a limited sample size. An unbiased  
538 sample is not representative of the whole population, and therefore, it is prudent that all available samples are used to fit the  
539 fragility functions.



540

541 **Fig. 11.** Fragility functions developed for manufacturing industry in (a) North Tohoku, (b) South Tohoku as well as food  
542 industry in (c) North Tohoku and (d) South Tohoku. To evaluate the effects of preceding earthquake damage on overall damage  
543 assessment, datasets for each industry were divided into North and South regions. Mean accuracies for each dataset were  
544 derived using a 10-fold cross-validation to determine if the accuracies of the fragility models are affected by the compound  
545 effect of earthquake and tsunamis.

## 546 9. Conclusions

### 547 9.1 Main findings and limitations

548 We presented a first attempt to quantifying structural vulnerability of port industries to tsunami impacts by developing a  
549 damage database for port structures and constructing damage fragility functions for various port industries. We were able to  
550 collect damage data for more than 5000 port structures and produce damage fragility functions for eight main port industries.  
551 Through the interpretations of our damage assessment and statistical analyses of our fragility model, a number of significant  
552 findings have emerged from this study:

- 553 1. Energy-related and warehousing and distribution industries showed relatively higher resistance to tsunami loads,  
554 whereas chemical, cargo handling and construction materials industry appeared to be more vulnerable.
- 555 2. Using our proposed damage classification scheme, our fragility models were able to reproduce damage with  
556 prediction accuracies of up to 75%, which outperforms models created using aggregated building damage data from  
557 MLIT (Leelawat et al., 2014).



558 3. Pre-tsunami earthquake activities have an influence on port structural damage. It is unavoidable that the compound  
559 effects of ground shaking and liquefaction are captured in the damage data, and unaccounted for in the process of  
560 developing fragility functions. However, ground shaking appears to influence building damage at lower damage  
561 states.

562 We are also aware of other limitations of this study. One of the limitations which has repeatedly surfaced in our findings is  
563 that inundation depth alone is not sufficient to explain the damage observed in port industries. Key threshold depths were  
564 difficult to capture for all industries which suggests that by only using inundation depth as a predictor, the fragility models  
565 may underestimate the levels of damage sustained by port structures. The models can be further refined by considering other  
566 measures of damage such as other tsunami flow characteristics (e.g. velocity, hydrodynamic force), debris impacts or the  
567 effects of shielding.

## 568 **9.2 Future use of damage database and recommendations**

569 This study presents an array of potential applications in future port damage studies. First and foremost, a new damage  
570 classification scheme was proposed to characterise damage to port structures. This scheme is transferable to other study sites  
571 for damage assessment and can be applied to damage assessments through ground survey, photographic interpretation, remote  
572 sensing and machine learning techniques. Secondly, we outlined a reproducible method for damage assessment in place of an  
573 actual ground survey, especially since this assessment was performed years after the event. The manual assessment allowed  
574 us to capture damage details from a side-profile, which otherwise would have been missing from automated techniques such  
575 as change detection in remote sensing imagery. In addition, the damage database can also be used in future work to investigate  
576 the influence of different parameters such as tsunami flow characteristics, construction characteristics and etcetera on the  
577 damage observed. Last but not least, our findings, quantified through the development of fragility functions, can be used to  
578 estimate damage to port structures in future tsunami events. They can also be used to motivate improvement in structural  
579 designs, tsunami mitigation measures as well as current methods of damage assessment. However, caution must be exercised  
580 when applying these models outside of Japan as structural integrity differs from place to place, though we expect that there  
581 would be less regional variability for port industries as compared to building codes in houses and commercial buildings.  
582 We invite and provide recommendations for potential users to expand the database and improve the predictive ability of the  
583 existing fragility models:

- 584 1. Expand the database by collecting damage data from other events and improve the quality of the database by providing  
585 more details on the (i) origin of tsunami, (ii) coastal morphological setting, and (iii) method of data collection.
- 586 2. Perform tsunami simulation to collect other intensity measures such as velocity and hydrodynamic force.
- 587 3. Study the performance of buildings and port infrastructure separately. This would, however, require a larger dataset  
588 than presented in this study because fragility models built on smaller sample sizes tend to have greater uncertainty.

589



590 **Data availability**

591 The database provides a comprehensive inventory of port structures and their associated damage in the 2011 Great East Japan  
592 tsunami. The database is available through an unrestricted data repository (DR-NTU) hosted by Nanyang Technological  
593 University (<https://doi.org/10.21979/N9/OTZMT1>) (Chua et al., 2020). A database guide is provided in the supplementary.

594

595 **Author contribution**

596 CTC designed the study, collected all data and information, performed all statistical analysis and prepared the manuscript.  
597 ADS provided direction for conceptualisation and advice on paper structure. AS provided the original MLIT damage data and  
598 provided guidance on the development of fragility functions. LL and KP provided advice on structural response and tsunami  
599 behaviour. DL provided advice for statistical analysis and development of fragility functions. IC provided advice on building  
600 damage assessment and development of damage database. TC provided advice for statistical analysis and developed code for  
601 bootstrapping techniques. AC assisted in the development of the damage database. SJ and NW provided general direction of  
602 paper. All authors contributed to the scientific discussion of the methods and results, as well as the editing of the manuscript.

603

604 **Competing interests**

605 The authors declare no competing interests.

606

607 **Acknowledgements**

608 This research was supported by the Earth Observatory of Singapore via its funding from the National Research Foundation  
609 Singapore and the Singapore Ministry of Education under the Research Centres of Excellence initiative. This work comprises  
610 EOS contribution number 329. The project was funded by SCOR Reinsurance Asia-Pacific. We are grateful for the support  
611 and advice we have received from Paul Nunn (SCOR Global P&C) and Nigel Winspear (formerly SCOR Global P&C). This  
612 work formed part of the PhD study of CTC, who received funding from the Nanyang Research Scholarship. This study was  
613 supported in part by the facilities and staff at the International Research Institute of Disaster Science (IRIDeS, Tohoku  
614 University). Special thanks go to Professor Fumihiko Imamura, the director of the International Research Institute of Disaster  
615 Science, for supporting and hosting the PhD student in IRIDeS. AS and KP were funded and supported by Tokio Marine &  
616 Nichido Fire Insurance Co., Ltd. and Willis Research Network (WRN). We would also like to thank Janneli Lea Soria, Stephen  
617 Chua and Jędrzej Majewski for providing feedback on the organisation of the manuscript.

618



## 619 References

- 620 Akiyama, M., Frangopol, D.M., Arai, M. and Koshimura, S.: Reliability of bridges under tsunami hazards: Emphasis on the  
621 2011 Tohoku-oki earthquake, *Earthquake Spectra*, 29, 295-314, <https://doi.org/10.1193/1.4000112>, 2013.
- 622 Ananth, C. V. and Kleinbaum, D. G.: Regression models for ordinal responses: a review of methods and applications,  
623 *International Journal of Epidemiology*, 26, 1323-1333, <http://doi.org/10.1093/ije/26.6.1323>, 1997.
- 624 Attary, N., Van De Lindt, J. W., Barbosa, A. R., Cox, D. T. and Unnikrishnan, V. U.: Performance-based tsunami engineering  
625 for risk assessment of structures subjected to multi-hazards: tsunami following earthquake, *Journal of Earthquake Engineering*,  
626 1-20 (2019).
- 627 Benazir, Syamsidik and Luthfi M.: Assessment on Damages of Harbor Complexes Due to Impacts of the 2018 Palu-Donggala  
628 Tsunami, Indonesia, in: *International Conference on Asian and Pacific Coasts*, edited by Nguyen, T. V., Dou, X. and Tran, T.  
629 T., Springer, Singapore, [https://doi.org/10.1007/978-981-15-0291-0\\_36](https://doi.org/10.1007/978-981-15-0291-0_36), 2019.
- 630 Building Centre of Japan: Introduction to Building Standard Law: Building Regulation in Japan,  
631 [https://www.bcj.or.jp/upload/international/baseline/BSLIntroduction201307\\_e.pdf](https://www.bcj.or.jp/upload/international/baseline/BSLIntroduction201307_e.pdf), last access: 15 October 2020, 2013.
- 632 Charvet, I., Ioannou, I., Rossetto, T., Suppasri, A. and Imamura, F.: Empirical fragility assessment of buildings affected by the  
633 2011 Great East Japan tsunami using improved statistical models, *Natural Hazards*, 73, 951-973,  
634 <https://doi.org/10.1007/s11069-014-1118-3>, 2014.
- 635 Charvet, I., Macabuag, J. and Rossetto, T.: Estimating tsunami-induced building damage through fragility functions: critical  
636 review and research needs, *Frontiers in Built Environment*, 3, 36, <https://doi.org/10.3389/fbuil.2017.00036>, 2017.
- 637 Charvet, I., Suppasri, A., Kimura, H., Sugawara, D. and Imamura, F.: A multivariate generalized linear tsunami fragility model  
638 for Kesennuma City based on maximum flow depths, velocities and debris impact, with evaluation of predictive accuracy,  
639 *Natural Hazards*, 79, 2073-2099, <https://doi.org/10.1007/s11069-015-1947-8>, 2015.
- 640 Chen, C., Melville, B. W., Nandasena, N. A. K., Shamseldin, A. Y. and Wotherspoon, L.: Experimental study of uplift loads  
641 due to tsunami bore impact on a wharf model, *Coastal Engineering*, 117, 126-137,  
642 <https://doi.org/10.1016/j.coastaleng.2016.08.001>, 2016.
- 643 Chua, C.T., Switzer, A.D., Suppasri, A., Li, L., Pakoksung, K., Lallemand, D., Jenkins, S., Charvet, I., Chua, T., Cheong, A.  
644 & Winspear, N.: Tsunami damage to ports: Cataloguing damage to create fragility functions from the 2011 Tohoku event,  
645 <https://doi.org/10.21979/N9/OTZMT1>, 2020.



- 646 Cruz, E. F., and Valdivia, D.: Performance of industrial facilities in the Chilean earthquake of 27 February 2010, The Structural  
647 Design of Tall and Special buildings, 20, 83-101, <https://doi.org/10.1002/tal.679>, 2011.
- 648 De Risi, R., Goda, K., Mori, N., and Yasuda, T.: Bayesian tsunami fragility modeling considering input data uncertainty,  
649 Stochastic Environmental Research and Risk Assessment, 31, 1253-1269, <https://doi.org/10.1007/s00477-016-1230-x>, 2017.
- 650 European Sea Ports Organisation: Trends in EU Ports Governance 2016.  
651 [https://www.espo.be/media/Trends\\_in\\_EU\\_ports\\_governance\\_2016\\_FINAL\\_VERSION.pdf](https://www.espo.be/media/Trends_in_EU_ports_governance_2016_FINAL_VERSION.pdf) last access: 23 October 2020,  
652 2016.
- 653 Fraser, S., Raby, A., Pomonis, A., Goda, K., Chian, S.C., Macabuag, J., Offord, M., Saito, K. and Sammonds, P.: Tsunami  
654 damage to coastal defences and buildings in the March 11th 2011 Mw 9.0 Great East Japan earthquake and tsunami, Bulletin  
655 of Earthquake Engineering, 11, 205-239, <https://doi.org/10.1007/s10518-012-9348-9>, 2013.
- 656 Geospatial Information Authority of Japan: Aerial photograph of the affected area.  
657 [https://www.gsi.go.jp/BOUSAI/h23\\_tohoku.html](https://www.gsi.go.jp/BOUSAI/h23_tohoku.html), last access: 23 October 2020, 2012a.
- 658 Geospatial Information Authority of Japan: Oblique photograph of the affected area.  
659 [https://www.gsi.go.jp/BOUSAI/h23\\_tohoku.html](https://www.gsi.go.jp/BOUSAI/h23_tohoku.html), last access: 23 October 2020, 2012b.
- 660 Geospatial Information Authority of Japan: Map/Aerial Photo Browsing Service. <http://mapps.gsi.go.jp/maplibSearch.do#1>,  
661 last access: 23 October 2020, 2013.
- 662 Gokon, H., Koshimura, S., Imai, K., Matsuoka, M., Namegaya, Y. and Nishimura, Y.: Developing fragility functions for the  
663 areas affected by the 2009 Samoa earthquake and tsunami. Natural Hazards and Earth System Sciences, 14, 3231,  
664 <https://doi.org/10.5194/nhess-14-3231-2014>, 2014.
- 665 Guisan, A. and Harrell, F. E.: Ordinal response regression models in ecology, Journal of Vegetation Science, 11, 617-626,  
666 <https://doi.org/10.2307/3236568>, 2000.
- 667 Hazarika, H., Kasama, K., Suetsugu, D., Kataoka, S., and Yasufuku, N.: Damage to geotechnical structures in waterfront areas  
668 of northern Tohoku due to the March 11, 2011 tsunami disaster, Indian Geotechnical Journal, 43, 137-152,  
669 <https://doi.org/10.1007/s40098-012-0021-7>, 2013.
- 670 Huang, J., and Chen, G.: Experimental modeling of wave load on a pile-supported wharf with pile breakwater, Ocean  
671 Engineering, 201, 107149, <https://doi.org/10.1016/j.oceaneng.2020.107149>, 2020.





- 672 Imai, K., Inazumi, T., Emoto, K., Horie, T., Suzuki, A., Kudo, K., Ogawa, M., Noji, M., Mizuto, K. and Sasaki, T.: Tsunami  
673 Vulnerability Criteria for Fishery Port Facilities in Japan, *Geosciences*, 9, 410, <https://doi.org/10.3390/geosciences9100410>,  
674 2019.
- 675 Janssen, H.: Study on the post-tsunami rehabilitation of fishing communities and fisheries-based livelihoods in Indonesia,  
676 International Collective in Support of Fishworkers, Banda Aceh/Jakarta, December 2005.
- 677 Japan Maritime Centre: The impact of the Great East Japan earthquake on the volume of seaborne cargo movement,  
678 [http://www.jpmac.or.jp/information/pdf/202\\_2.pdf](http://www.jpmac.or.jp/information/pdf/202_2.pdf) , last access: 20 September 2020, 2011.
- 679 Karafagka, S., Fotopoulou, S. and Ptilakis, K.: Analytical tsunami fragility curves for seaport RC buildings and steel light  
680 frame warehouses, *Soil Dynamics and Earthquake Engineering*, 112, 118-137, <https://doi.org/10.1016/j.soildyn.2018.04.037>,  
681 2018.
- 682 Kazama, M. and Noda, T.: Damage statistics (Summary of the 2011 off the Pacific Coast of Tohoku Earthquake damage),  
683 *Soils and Foundations*, 52, 780-792, <http://doi.org/10.1016/j.sandf.2012.11.003>, 2012.
- 684 Kihara, N., Niida, Y., Takabatake, D., Kaida, H., Shibayama, A. and Miyagawa, Y.: Large-scale experiments on tsunami-  
685 induced pressure on a vertical tide wall, *Coastal engineering*, 99, 46-63, <https://doi.org/10.1016/j.coastaleng.2015.02.009>,  
686 2015.
- 687 Koshimura, S., Namegaya, Y. and Yanagisawa, H.: Tsunami fragility: A new measure to identify tsunami damage, *Journal of*  
688 *Disaster Research*, 4, 479-488, <https://doi.org/10.20965/jdr.2009.p0479>, 2009.
- 689 Krausmann, E. and Cruz, A. M.: Impact of the 11 March 2011, Great East Japan earthquake and tsunami on the chemical  
690 industry, *Natural hazards*, 67, 811-828, <https://doi.org/10.1007/s11069-013-0607-0>, 2013.
- 691 Lallemand, D., Kiremidjian, A., and Burton, H.: Statistical procedures for developing earthquake damage fragility curves,  
692 *Earthquake Engineering and Structural Dynamics*, 44, 1373-1389, <https://doi.org/10.1002/eqe.2522>, 2015.
- 693 Lam, J. S. L. and Lassa, J. A.: Risk assessment framework for exposure of cargo and ports to natural hazards and climate  
694 extremes. *Maritime Policy and Management*, 44, 1-15, <https://doi.org/10.1080/03088839.2016.1245877>, 2017.
- 695 Leelawat, N., Suppasri, A., Charvet, I. and Imamura, F.: Building damage from the 2011 Great East Japan tsunami: quantitative  
696 assessment of influential factors, *Natural Hazards*, 73, 449-471, <https://doi.org/10.1007/s11069-014-1081-z>, 2014.



- 697 Leelawat, N., Suppasri, A., Murao, O. and Imamura, F.: A study on the influential factors on building damage in Sri Lanka  
698 during the 2004 Indian Ocean tsunami, *Journal of Earthquake and Tsunami*, 10, 1640001,  
699 <https://doi.org/10.1142/S1793431116400017>, 2016.
- 700 Leone, F., Lavigne, F., Paris, R., Denain, J. C. and Vinet, F.: A spatial analysis of the December 26th, 2004 tsunami-induced  
701 damages: Lessons learned for a better risk assessment integrating buildings vulnerability, *Applied Geography*, 31, 363-375,  
702 <https://doi.org/10.1016/j.apgeog.2010.07.009>, 2011.
- 703 Li, L., Switzer, A. D., Wang, Y., Chan, C. H., Qiu, Q., and Weiss, R.: A modest 0.5-m rise in sea level will double the tsunami  
704 hazard in Macau. *Science Advances*, 4, eaat1180, <https://doi.org/10.1126/sciadv.aat1180>, 2018.
- 705 Macabuag, J., Rossetto, T., Ioannou, I., Suppasri, A., Sugawara, D., Adriano, B., Imamura, F., Eames, I. and Koshimura, S.:  
706 A proposed methodology for deriving tsunami fragility functions for buildings using optimum intensity measures, *Natural  
707 Hazards*, 84, 1257-1285, <https://doi.org/10.1007/s11069-016-2485-8>, 2016.
- 708 Maheshwari, B. K., Sharma, M. L. and Narayan, J. P.: Structural damages on the coast of Tamil Nadu due to tsunami caused  
709 by December 26, 2004 Sumatra earthquake, *ISET Journal of Earthquake Technology*, 42, 3, 2005.
- 710 Mas E, Koshimura S, Suppasri A, Matsuoka M, Matsuyama M, Yoshii T, Jimenez C, Yamazaki F, Imamura F.: Developing  
711 Tsunami fragility curves using remote sensing and survey data of the 2010 Chilean Tsunami in Dichato, *Natural Hazards and  
712 Earth System Sciences*, 12, 2689-2697, <https://doi.org/10.5194/nhess-12-2689-2012>, 2012.
- 713 Meneses, J. and Arduino, P.: Preliminary observations of the effects of ground failure and tsunami on the major ports of Ibaraki  
714 prefecture, GEER Assoc. Rep. No. GEER-025c, 2011.
- 715 Ministry of Land Infrastructure and Transportation (MLIT): Investigation of the impact on business activities due to the  
716 suspension of port functions in the Great East Japan Earthquake: Questionnaire survey results.  
717 [http://www.thr.mlit.go.jp/bumon/kisya/kisyah/images/38985\\_1.pdf](http://www.thr.mlit.go.jp/bumon/kisya/kisyah/images/38985_1.pdf), last access: 15 September 2020, 2011.
- 718 Ministry of Land Infrastructure and Transportation (MLIT): Survey of tsunami damage condition,  
719 <http://www.mlit.go.jp/toshi/toshi-hukkou-arkaibu.html>, last access: 23 October 2020, 2014.
- 720 Muhari, A., Charvet, I., Tsuyoshi, F., Suppasri, A. and Imamura, F.: Assessment of tsunami hazards in ports and their impact  
721 on marine vessels derived from tsunami models and the observed damage data, *Natural Hazards*, 78, 1309-1328,  
722 <https://doi.org/10.1007/s11069-015-1772-0>, 2015.



- 723 Nayak, S., Reddy, M. H. O., Madhavi, R. and Dutta, S. C.: Assessing tsunami vulnerability of structures designed for seismic  
724 loading, *International Journal of Disaster Risk Reduction*, 7, 28-38, <https://doi.org/10.1016/j.ijdr.2013.12.001>, 2014.
- 725 Nistor, I., Palermo, D., Nouri, Y., Murty, T. and Saatcioglu, M.: Tsunami-induced forces on structures, in: *Handbook of coastal*  
726 *and ocean engineering*, edited by Kim, C.Y., World Scientific, Singapore, 261-286 ,  
727 [https://doi.org/10.1142/9789812819307\\_0011](https://doi.org/10.1142/9789812819307_0011), 2010.
- 728 Okazaki, T., Lignos, D. G., Midorikawa, M., Ricles, J. M., and Love, J.: Damage to steel buildings observed after the 2011  
729 Tohoku-Oki earthquake, *Earthquake Spectra*, 29, 219-243, <https://doi.org/10.1193/1.4000124>, 2013.
- 730 Otake, T., Suppasri, A. and Imamura, F.: Investigations on global tsunami risk considering port network, *JSCE Proceedings*  
731 *B2 (Coastal Engineering)*, 75, 1884-2399, [https://doi.org/10.2208/kaigan.75.I\\_1321](https://doi.org/10.2208/kaigan.75.I_1321) , 2019 [in Japanese].
- 732 Ozawa, S., Nishimura, T., Suito, H., Kobayashi, T., Tobita, M. and Imakiire, T.: Coseismic and postseismic slip of the 2011  
733 magnitude-9 Tohoku-Oki earthquake, *Nature*, 475, 373-376, <https://doi.org/10.1038/nature10227>, 2011.
- 734 Park, H., Cox, D. T. and Barbosa, A. R.: Comparison of inundation depth and momentum flux based fragilities for probabilistic  
735 tsunami damage assessment and uncertainty analysis, *Coastal Engineering*, 122, 10-26,  
736 <https://doi.org/10.1016/j.coastaleng.2017.01.008>, 2017.
- 737 Paulik, R., Gusman, A., Williams, J.H., Pratama, G.M., Lin, S.L., Prawirabhakti, A., Sulendra, K., Zachari, M.Y., Fortuna,  
738 Z.E.D., Layuk, N.B.P. and Suwarni, N.W.I.: Tsunami hazard and built environment damage observations from Palu City after  
739 the September 28 2018 Sulawesi earthquake and tsunami, *Pure and Applied Geophysics*, 176, 3305-3321,  
740 <https://doi.org/10.1007/s00024-019-02254-9>, 2019.
- 741 Percher, M. Bruin, W., Dickenson, S. and Eskijian, M.: Performance of port and harbor structures impacted by the March 11,  
742 2011 Great Tohoku Earthquake and Tsunami, in: *Ports 2013: Success Through Diversification*, 610-619,  
743 <http://doi/10.1061/9780784413067.063>, 2013.
- 744 Pitilakis, K., Crowley, H. and Kaynia, A. M.: Introduction, in: *SYNER-G: Typology Definition and Fragility Functions for*  
745 *Physical Elements at Seismic Risk*, 1-28, Springer, Dordrecht, <http://doi.org/10.1007/978-94-007-7872-6>, 2014.
- 746 R Core Team: R: A language and environment for statistical computing, R Foundation for Statistical Computing, Vienna,  
747 Austria. <https://www.R-project.org/>, 2020.



- 748 Reese, S., Bradley, B.A., Bind, J., Smart, G., Power, W. and Sturman, J.: Empirical building fragilities from observed damage  
749 in the 2009 South Pacific tsunami, *Earth-Science Reviews*, 107, 156-173, <https://doi.org/10.1016/j.earscirev.2011.01.009>,  
750 2011.
- 751 Rossetto, T., Ioannou, I., Grant, D. N. and Maqsood, T.: Guidelines for empirical vulnerability assessment, in: GEM technical  
752 report, GEM Foundation, Pavia, 2014.
- 753 Scawthorn, C., Ono, Y., Iemura, H., Ridha, M. and Purwanto, B.: Performance of lifelines in Banda Aceh, Indonesia, during  
754 the December 2004 Great Sumatra earthquake and tsunami. *Earthquake Spectra*, 22, 511-544,  
755 <https://doi.org/10.1193/1.2206807>, 2006.
- 756 Shoji, G. and Nakamura, T.: Damage assessment of road bridges subjected to the 2011 Tohoku Pacific earthquake tsunami,  
757 *Journal of Disaster Research*, 12, 79-89, <https://doi.org/10.20965/jdr.2017.p00792>, 2017.
- 758 Song, J., De Risi, R. and Goda, K.: Influence of flow velocity on tsunami loss estimation, *Geosciences*, 7, 114,  
759 <https://doi.org/10.3390/geosciences7040114>, 2017.
- 760 Sugano, T., Nozu, A., Kohama, E., Shimosako, K. I. and Kikuchi, Y.: Damage to coastal structures, *Soils and Foundations*,  
761 54, 883-901, <https://doi.org/10.1016/j.sandf.2014.06.018>, 2014.
- 762 Suppasri, A., Charvet, I., Imai, K. and Imamura, F.: Fragility curves based on data from the 2011 Tohoku-Oki Tsunami in  
763 Ishinomaki city, with discussion of parameters influencing building damage, *Earthquake Spectra*, 31, 841-868,  
764 <https://doi.org/10.1193/053013EQS138M>, 2015.
- 765 Suppasri, A., Mas, E., Charvet, I., Gunasekera, R., Imai, K., Fukutani, Y., Abe, Y. and Imamura, F.: Building damage  
766 characteristics based on surveyed data and fragility curves of the 2011 Great East Japan tsunami, *Natural Hazards*, 66, 319-  
767 341, <https://doi.org/10.1007/s11069-012-0487-8>, 2013.
- 768 Suppasri, A., Pakoksung, K., Charvet, I., Chua, C. T., Takahashi, N., Ornthammarath, T., Latcharote, P., Leelawat, N., and  
769 Imamura, F.: Load-resistance analysis: an alternative approach to tsunami damage assessment applied to the 2011 Great East  
770 Japan tsunami, *Nat. Hazards Earth Syst. Sci.*, 19, 1807–1822, <https://doi.org/10.5194/nhess-19-1807-2019>, 2019.
- 771 Takano, T.: Overview of the 2011 East Japan earthquake and tsunami disaster, 2011.
- 772 Tarbotton, C., Dall'Osso, F., Dominey-Howes, D., and Goff, J.: The use of empirical vulnerability functions to assess the  
773 response of buildings to tsunami impact: comparative review and summary of best practice, *Earth-science reviews*, 142, 120-  
774 134, <https://doi.org/10.1016/j.earscirev.2015.01.002>, 2015.



- 775 Technical Council on Lifeline Earthquake Engineering: Ports, in: Tohoku, Japan, Earthquake and Tsunami of 2011: Lifeline  
776 Performance, edited by Tang, A.K., American Society of Civil Engineers, 547-558,  
777 <https://doi.org/10.1061/9780784479834.ch07>, 2013.
- 778 The 2011 Tohoku Earthquake Tsunami Joint Survey Group.: The 2011 off the Pacific coast of Tohoku earthquake tsunami  
779 information—field survey results, Coastal Engineering Committee of the Japan Society of Civil Engineers,  
780 <https://coastal.jp/tsunami2011/> (2011).
- 781 Tsuji, Y., Satake, K., Ishibe, T., Harada, T., Nishiyama, A. and Kusumoto, S.: Tsunami heights along the pacific coast of  
782 northern Honshu recorded from the 2011 Tohoku and previous great earthquakes, Pure and Applied Geophysics, 171, 3183-  
783 3215, <https://doi.org/10.1007/s00024-014-0779-x>, 2014.
- 784 United States Geological Survey: M 9.1 - 2011 Great Tohoku Earthquake, Japan.  
785 [https://earthquake.usgs.gov/earthquakes/eventpage/official20110311054624120\\_30/shakemap/intensity](https://earthquake.usgs.gov/earthquakes/eventpage/official20110311054624120_30/shakemap/intensity) , last access: 16  
786 October 2020, 2020.
- 787 Williams, J.H., Wilson, T.M., Horspool, N., Paulik, R., Wotherspoon, L., Lane, E.M. and Hughes, M.W.: Assessing  
788 transportation vulnerability to tsunamis: Utilising post-event field data from the 2011 Tōhoku tsunami, Japan, and the 2015  
789 Illapel tsunami, Chile, Natural Hazards and Earth System Sciences, 20, 451–470, <https://doi.org/10.5194/nhess-20-451-2020>,  
790 2020.
- 791 Yung, Y. F., and Bentler, P. M.: Bootstrapping techniques in analysis of mean and covariance structures, Advanced structural  
792 equation modeling: Issues and techniques, 195-226, 1996.